

Chalcogenide glass microlenses by inkjet printing

Eric A. Sanchez, Maike Waldmann, and Craig B. Arnold*

Princeton Institute for the Science and Technology of Materials,
Princeton University, Princeton, New Jersey 08540, USA

*Corresponding author: cbarnold@princeton.edu

Received 25 January 2011; accepted 27 February 2011;
posted 23 March 2011 (Doc. ID 139713); published 4 May 2011

We demonstrate micrometer scale mid-IR lenses for integrated optics, using solution-based inkjet printing techniques and subsequent processing. Arsenic sulfide spherical microlenses with diameters of 10–350 μm and focal lengths of 10–700 μm have been fabricated. The baking conditions can be used to tune the precise focal length. © 2011 Optical Society of America

OCIS codes: 080.3630, 130.3990, 130.3130, 130.3060, 160.2750, 220.4000.

1. Introduction

Mid-IR (MIR) technology has emerged as a constantly growing market over the past decade. While formerly used for materials processing and medical procedures mainly, MIR technology is now a major part of current research in sensing and military applications, as well as wireless communication [1–4]. This development has been further encouraged by the success of tailor-made quantum cascade lasers emitting at user-defined MIR frequencies [5]. However, in order to use this particular spectral range efficiently, optical materials and structures that are transparent in the MIR are needed to focus and direct the light. Therefore, the MIR-transparent chalcogenide glasses, such as amorphous arsenic sulfide (As_2S_3) which has a long wavelength cutoff at 9.4 μm [6], have evoked an increasing interest to be used as optics in the MIR [7–9]. Chalcogenide glass thin films and waveguides for optical devices are fabricated either by vapor-phase or solution-based processing, the former technique leading to amorphous thin films, which can then be structured by various lithographic techniques to obtain waveguides [10,11], and the latter technique leading directly to complex waveguide geometries [6,12–14]. However, optical devices, such as lenses with geometries that deviate strongly from conventional waveguides, have to be

fabricated individually, which becomes increasingly troublesome with decreasing size [15,16]. Hisakuni and Tanaka demonstrated microlenses on the surface of thick As_2S_3 films using local photoexpansion caused by laser illumination [17]. Ma *et al.* showed a molding process to obtain lens arrays in a chalcogenide glass disk [18]. However, neither of these techniques allows for direct deposition of single lenses onto user-defined surfaces. In contrast, inkjet printing techniques have been used to directly print microlenses for the visible spectral range [19–23]. In this paper, we introduce inkjet printing of chalcogenide glass solutions to fabricate spherical lenses of 10–350 μm in diameter for the MIR, the smallest lenses being the size scale of a quantum cascade laser facet [6].

2. Experimental

The chalcogenide glass lenses are fabricated by dispensing small amounts of an As_2S_3 solution on a hydrophobic substrate surface. Two different As_2S_3 solutions are made from either 2 g or 4 g amorphous bulk As_2S_3 (Strem Chemicals, Inc., 99.9%) dissolved for seven days in 20 ml *n*-propylamine (Sigma-Aldrich, p.a.) in sealed amber glass bottles [24]. The solutions are mixed and stored under nitrogen atmosphere in order to avoid exposure to ambient moisture [25]. The substrates are indium phosphide (AXT, Inc.) wafers that have been treated with 10% hydrofluoric acid for 10 s prior to being used in order to

Table 1. Fabrication Parameters and Resulting Lens Geometry (lens diameter and height measured by profilometry) of Microlenses on Indium Phosphide Substrates after 8 h Baking

Inkjet Technique	Voltage	Pulse Length	Solution Concentration	Lens Diameter	Lens Height	Calculated Focal Length
Piezoelectric	80 V	30 μ s	2 g/20 ml	11.0 \pm 0.6 μ m	0.8 \pm 0.2 μ m	13.8 \pm 5.1 μ m
Piezoelectric	90 V	30 μ s	4 g/20 ml	12.1 \pm 0.6 μ m	1.2 \pm 0.3 μ m	11.3 \pm 4.0 μ m
Piezoelectric	80 V	40 μ s	2 g/20 ml	20.3 \pm 0.6 μ m	1.9 \pm 0.3 μ m	20.0 \pm 4.2 μ m
Piezoelectric	97 V	40 μ s	4 g/20 ml	20.2 \pm 0.7 μ m	2.8 \pm 0.5 μ m	14.0 \pm 3.2 μ m
Piezoelectric	97 V	45 μ s	4 g/20 ml	30.1 \pm 1.6 μ m	12.3 \pm 1.7 μ m	11.0 \pm 1.0 μ m
Pneumatic	-	10 ms	4 g/20 ml	135 \pm 6.4 μ m	14.5 \pm 1.8 μ m	118 \pm 24 μ m
Pneumatic	-	50 ms	4 g/20 ml	330 \pm 2.7 μ m	31.2 \pm 2.3 μ m	325 \pm 18 μ m

remove surface native oxide, and thus increase hydrophobicity and reduce wettability [26].

We used two different types of inkjet setups to dispense the solutions on the substrates. One is a manually operated pneumatic system (EFD, Inc.), while the other is a computer-controlled piezoelectric system (Microdrop Technologies, GmbH). In the pneumatic system, 30 μ l of the As₂S₃ solution are placed in a reservoir, which has a dispensing tip attached. The tip has an aperture diameter of 130 μ m and is placed approximately 0.25 mm above the substrate surface. By applying a differential pressure of 3.4 kPa for 10–52 ms, the solution forms a jet and is deposited on the substrate. In the piezoelectric system, 10 μ l of the As₂S₃ solution are loaded in a glass capillary, which has an aperture diameter of 50 μ m at the tip. The tip is placed approximately 0.5 mm above the substrate surface. By applying a voltage of 80–150 V for 30–45 μ s to the piezoelectric actuator, a differential pressure of about 3.5 MPa causes a jet of the solution to form which deposits drops on the substrate.

After depositing the As₂S₃ solution drops on the substrate, they must undergo heat treatment in order to densify the glass and to remove residual solvent [24]. Therefore, the samples are transferred to a vacuum oven immediately after drop deposition, and are baked under vacuum for 2–8 h at 66 °C. During and after baking, the samples are kept in the dark to avoid exposure to ambient light, which is known to affect the optical properties of chalcogenide glass [27].

The curvature and contact angle of the as-deposited drops are measured by taking photographs with a CCD camera (Tokyo Electronic Industry, Co.) of the lens profile and interpreting the images. The lens diameter, height, and curvature of the baked lenses are measured by a stylus profilometer (KLA-Tencor, Co.) and a three-dimensional (3D) measuring laser microscope (Olympus). In order to determine the focal length of large diameter lenses, a collimated laser beam (532 nm) passes the lens, and the distance between lens and focal point is measured.

3. Results

By using inkjet printing, we are able to make chalcogenide glass microlenses in the range of 10–350 μ m in diameter and 0.8–22 μ m in height. The piezoelectric setup covers the lower end of the size spectrum up to 30 μ m lens diameter, while the pneumatic setup

works well for larger lenses. Table 1 shows typical lens properties of lenses which have been made using different fabrication parameters. All lenses have been baked for 8 h. For each set of fabrication parameters, diameters and heights of 8–10 lenses have been averaged in order to determine the mean value and the standard deviation.

The lenses exhibit spherical geometry, as shown in Fig. 1, which they retain during the baking. Figure 1(a) shows a 3D scan of a large lens (lens diameter of 330 μ m) taken with a laser microscope after baking. The upper graph in Fig. 1(b) shows the height profile through the center of the same lens. For comparison, a profilometry scan across the height of a small lens (lens diameter of 16 μ m) is shown in the lower graph. Both profiles can be fitted to part of a circle with diameters of 2.07 mm and 21 μ m, respectively.

The curvature of the lenses depends on the contact angle of the deposited drop on the substrate surface.

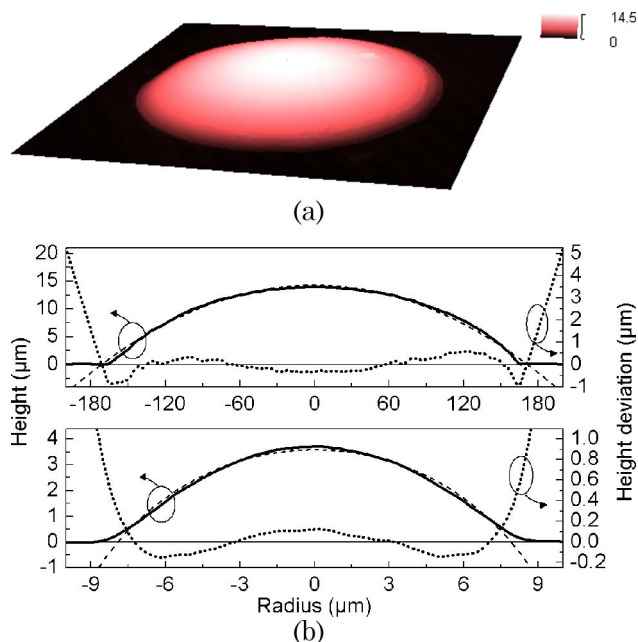


Fig. 1. (Color online) (a) 3D laser microscope scan of a large microlens (330 μ m in diameter). Note that the vertical and the horizontal scales are different. (b) Height profile of a large microlens (upper graph) corresponding to (a). Dashed curve shows fit to circle of 2.07 mm in diameter. Lower graph shows the height profile of a small microlens (16 μ m in diameter) measured by profilometry and fit to a circle of 21 μ m in diameter (dashed curve). The dotted curves show the height deviation of the circular fit functions.

Figure 2(a) shows a drop of the less concentrated solution on a nontreated substrate surface. Since the solution is highly polar, it spreads widely on the hydrophilic surface, producing a contact angle of 6.6° . On the other hand, Fig. 2(b) shows a substrate surface that has been treated with hydrofluoric acid to remove the native oxide, producing a hydrophobic layer which leads to a contact angle significantly higher of 21.7° . Therefore, a hydrophobic substrate surface leads to a smaller radius of curvature, which goes hand-in-hand with a shorter focal length.

By baking the lenses, the geometry and the refractive index can be adjusted. Heat treatment of solution-processed As_2S_3 leads to the removal of residual solvent and densification. Therefore, the volume changes, resulting in a decrease of lens height. Lens diameter and spherical geometry are retained during the baking, which is why the curvature decreases while the focal length increases. By measuring the focal length and the decrease of the lens height, we can easily determine the refractive index of the lens, which also changes with baking duration. A spherical cap can be described by

$$\frac{1}{R} = \frac{2h}{r^2 + h^2}, \quad (1)$$

where R is the spherical radius, r and h the radius and height of the lens, respectively. The focal length of a plano-convex lens is given by

$$f = \frac{R}{n - 1}, \quad (2)$$

where n is the wavelength-dependent refractive index of the lens. Combining these two equations leads to

$$f = \frac{r^2 + h^2}{2h(n - 1)} \quad \text{or} \quad n = 1 + \frac{r^2 + h^2}{2hf}. \quad (3)$$

However, due to the solvent evaporation and densification during heat treatment, the height h changes, as do the focal length and the refractive index, which has to be accounted for. By introducing the relative height, $\beta(t) = \frac{h}{h_0}$, Eq. (3) changes to

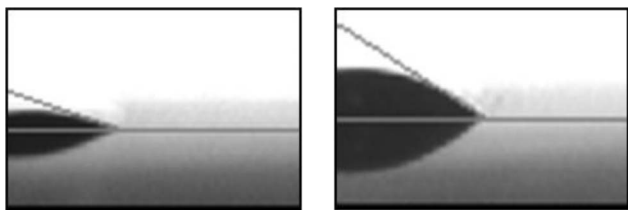


Fig. 2. (a) Contact angle of arsenic sulfide solution on nontreated (6.6°) and (b) on hydrofluoric acid treated (21.7°) indium phosphide substrate surface.

$$f(t) = \frac{r^2 + [\beta(t)h_0]^2}{2\beta(t)h_0[n(t) - 1]}, \quad (4)$$

where h_0 is the initial height of the as-deposited lens.

Figure 3 shows the relative height $\beta(t)$ for the two different solutions. For each solution relative heights of eight lenses have been determined by taking images with the CCD camera and averaged in order to determine the mean value and the standard deviation. The standard deviations are small compared to the uncertainties of the height measurement according to the pixel resolution of the CCD camera (uncertainty $2.5\mu\text{m}$). The solution with the lower As_2S_3 concentration has been deposited on hydrofluoric acid treated substrates, while nontreated substrates have been used for the solution with the higher concentration. Lenses made from the two different solutions show similar behavior: After a fast lens height decrease, the shrinkage saturates at a constant value. Lenses made of the less concentrated solution shrink more considerably, since they start with a higher solvent fraction which they gradually lose. After six hours baking, their height decreases by more than 70%, while lenses that are made from the higher concentrated solution only decrease by 50% in height. After baking is completed and the samples are returned to room temperature, there is no subsequent change in height anymore. Thus, using a certain solution concentration and baking duration gives us a means to tailor the final focal length of the lenses.

For lens diameters greater than 1 mm, we can directly measure the focal length using optical techniques described earlier. Accordingly, the data of six large diameter lenses (diameters of 1.6–5.0 mm) as a function of the baking duration is presented in Fig. 4, normalized by the lens diameter and averaged. The normalization gives us the f -number: $f\text{-number} = f/d$. The f -number increases monotonically, approaching saturation at long baking durations. By measuring the lens height h and the focal length f over baking time, as well as the lens

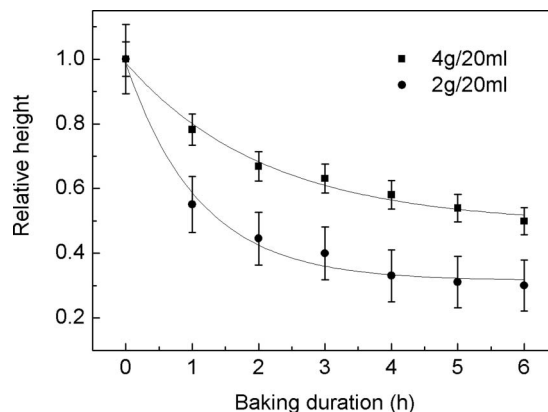


Fig. 3. CCD camera measurements of the relative height for lenses made from two different arsenic sulfide solutions depending on the baking duration. Error bars indicate the measurement uncertainty. Curves serve as guide to the eye only.

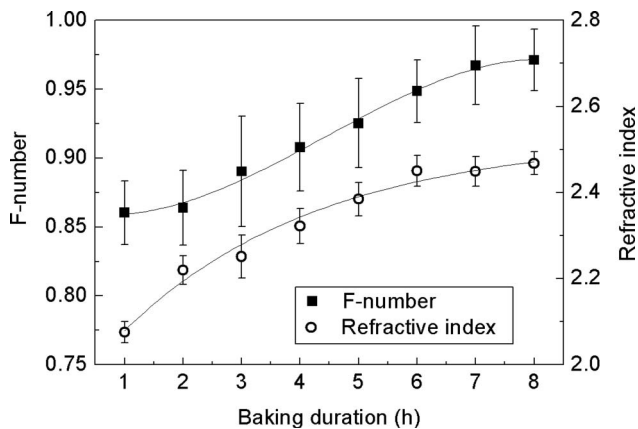


Fig. 4. F -number and refractive index of large lenses (1.5–5 mm diameter) versus baking duration. F -number is the focal length divided by the lens diameter; refractive index is measured at 532 nm and averaged. Error bars indicate standard deviation. Curves serve as guide to the eye only.

radius r , which is constant, the refractive index n can be determined using Eq. (3). The focal length measurements are conducted in the visible range with a measurement resolution of $50\ \mu\text{m}$. The dispersion relation for this material has been studied earlier [24], and allows one to extrapolate the index into the MIR spectral range if needed. Figure 4 shows that at short baking durations, the refractive index increases rapidly, approaching saturation at a value of 2.4 after seven hours of baking. Only after these relatively long times are the values in agreement with the previous measurements of the refractive index as a function of baking parameters made on As_2S_3 thin films [24]. This is due to the different geometry of a lens compared to a thin film. In [24], constancy of the refractive index is reached after over 20 h at a baking temperature of $90\ ^\circ\text{C}$. Since the focal length reaches constancy as soon as lens height and refractive index are constant over baking time, we expect the focal length to reach complete saturation at baking durations over at least 20 h. In this time frame, the focal length can be easily adjusted.

For smaller lenses, this optical measurement technique is not sensitive and so we need to calculate the focal length based on the calculated index of refraction of large lenses which have been fabricated with the same solution and baking parameters. This is done by using Eq. (4), and the data for the averaged focal lengths is presented in Table 1.

The lenses in Table 1, which have been fabricated with the piezoelectric setup exhibit focal lengths between 10 and $20\ \mu\text{m}$, and the lenses made by the pneumatic setup show focal lengths of 100 and $700\ \mu\text{m}$, respectively. By choosing a certain substrate surface treatment, solution concentration, drop size, and baking duration, the lens geometry can be tailored for various applications.

4. Conclusion

We have shown a reliable fabrication technique for chalcogenide glass microlenses on arbitrary

hydrophobic substrates. By combining solution-based processing of chalcogenide glass and different inkjet printing techniques, we demonstrate spherical chalcogenide glass microlenses $10\text{--}350\ \mu\text{m}$ in diameter with focal lengths of $10\text{--}700\ \mu\text{m}$. The dimensions of the smallest microlenses are in the same range as the size of a quantum cascade laser ridge opening the door to novel implementations of these integrated optics.

This work was supported by National Science Foundation (NSF) grant EEC-0540832 through the Center of Mid-Infrared Technologies for Health and the Environment. E. Sanchez acknowledges the Louis Stokes Alliance for Minority Participation for financial support. M. Waldmann acknowledges the German Academic Exchange Service for generous support within the postdoctoral fellowship program. The authors thank Shanshan Song and Candice Tsay for mechanical profilometry measurements on the samples and valuable discussion.

References

1. C. Gmachl, F. Capasso, D. L. Sivco, and A. Y. Cho, "Recent progress in quantum cascade lasers and applications," *Rep. Prog. Phys.* **64**, 1533–1601 (2001).
2. K. Karstad, A. Stefanov, M. Wegmuller, H. Zbinden, N. Gisin, T. Aellen, M. Beck, and J. Faist, "Detection of mid-IR radiation by sum frequency generation for free space optical communication," *Opt. Lasers Eng.* **43**, 537–544 (2005).
3. A. Kosterev and F. Tittel, "Chemical sensors based on quantum cascade lasers," *IEEE J. Quantum Electron.* **38**, 582–591 (2002).
4. Z. Yin and X. Tang, "A review of energy bandgap engineering in iii-v semiconductor alloys for mid-infrared laser applications," *Solid-State Electron.* **51**, 6–15 (2007).
5. F. Capasso, C. Gmachl, R. Paiella, A. Tredicucci, A. Hutchinson, D. Sivco, J. Baillargeon, A. Cho, and H. Liu, "New frontiers in quantum cascade lasers and applications," *IEEE J. Sel. Top. Quantum Electron.* **6**, 931–947 (2000).
6. C. Tsay, E. Mujagic, C. K. Madsen, C. F. Gmachl, and C. B. Arnold, "Mid-infrared characterization of solution-processed As_2S_3 chalcogenide glass waveguides," *Opt. Express* **18**, 15523–15530 (2010).
7. V. Ta'eed, N. J. Baker, L. Fu, K. Finsterbusch, M. R. E. Lamont, D. J. Moss, H. C. Nguyen, B. J. Eggleton, D.-Y. Choi, S. Madden, and B. Luther-Davies, "Ultrafast all-optical chalcogenide glass photonic circuits," *Opt. Express* **15**, 9205–9221 (2007).
8. L. Labadie and O. Wallner, "Mid-infrared guided optics: a perspective for astronomical instruments," *Opt. Express* **17**, 1947–1962 (2009).
9. A. Zakery and S. R. Elliott, "Optical properties and applications of chalcogenide glasses: a review," *J. Non-Cryst. Solids* **330**, 1–12 (2003).
10. A. Ganjoo, H. Jain, C. Yu, R. Song, J. Ryan, J. Irudayaraj, Y. Ding, and C. Pantano, "Planar chalcogenide glass waveguides for IR evanescent wave sensors," *J. Non-Cryst. Solids* **352**, 584–588 (2006).
11. S. J. Madden, T. Han, D. A. Bulla, and B. Luther-Davies, "Low loss chalcogenide glass waveguides fabricated by thermal nanoimprint lithography," in *Optical Fiber Communication Conference* (Optical Society of America, 2010), paper OMH3.
12. C. Tsay, F. Toor, C. F. Gmachl, and C. B. Arnold, "Chalcogenide glass waveguides integrated with quantum cascade lasers for

- on-chip mid-IR photonic circuits,” *Opt. Lett.* **35**, 3324–3326 (2010).
13. C. Tsay, Y. Zha, and C. B. Arnold, “Solution-processed chalcogenide glass for integrated single-mode mid-infrared waveguides,” *Opt. Express* **18**, 26744–26753 (2010).
 14. A. Zoubir, M. Richardson, C. Rivero, A. Schulte, C. Lopez, K. Richardson, N. Hô, and R. Vallée, “Direct femtosecond laser writing of waveguides in As_2S_3 thin films,” *Opt. Lett.* **29**, 748–750 (2004).
 15. H. Hisakuni and K. Tanaka, “Optical microfabrication of chalcogenide glasses,” *Science* **270**, 974–975 (1995).
 16. H. Ottevaere, R. Cox, H. P. Herzig, T. Miyashita, K. Naessens, M. Taghizadeh, R. Völkel, H. J. Woo, and H. Thienpont, “Comparing glass and plastic refractive microlenses fabricated with different technologies,” *J. Opt. A Pure Appl. Opt.* **8**, S407–S429 (2006).
 17. H. Hisakuni and K. Tanaka, “Optical fabrication of microlenses in chalcogenide glasses,” *Opt. Lett.* **20**, 958–960 (1995).
 18. K. J. Ma, H. H. Chien, S. W. Huang, W. Y. Fu, and C.-L. Chao, “Contactless molding of arrayed chalcogenide glass lenses,” *J. Non-Cryst. Solids* (to be published).
 19. S. Biehl, R. Danzebrink, P. Oliveira, and M. Aegerter, “Refractive microlens fabrication by ink-jet process,” *J. Sol-Gel Sci. Technol.* **13**, 177–182 (1998).
 20. D. MacFarlane, V. Narayan, J. Tatum, W. Cox, T. Chen, and D. Hayes, “Microjet fabrication of microlens arrays,” *IEEE Photon. Technol. Lett.* **6**, 1112–1114 (1994).
 21. E. Bonaccorso, H.-J. Butt, B. Hankeln, B. Niesenhaus, and K. Graf, “Fabrication of microvessels and microlenses from polymers by solvent droplets,” *Appl. Phys. Lett.* **86**, 124101 (2005).
 22. F.-C. Chen, J.-P. Lu, and W.-K. Huang, “Using ink-jet printing and coffee ring effect to fabricate refractive microlens arrays,” *IEEE Photon. Technol. Lett.* **21**, 648–650 (2009).
 23. Y. S. Yang, D.-H. Youn, S. H. Kim, S. C. Lim, H. S. Shim, S. Y. Kang, and I.-K. You, “Preparation and characteristics of pmma microlens array for a blu application by an inkjet printing method,” *Mol. Cryst. Liq. Cryst.* **520**, 239–244 (2010).
 24. S. Song, J. Dua, and C. B. Arnold, “Influence of annealing conditions on the optical and structural properties of spin-coated As_2S_3 chalcogenide glass thin films,” *Opt. Express* **18**, 5472–5480 (2010).
 25. G. C. Chern and I. Lauks, “Spin-coated amorphous chalcogenide films,” *J. Appl. Phys.* **53**, 6979–6982 (1982).
 26. H. Zhao, L. Yu, and Y. Huang, “Investigation of a chemically treated $inp(1\text{Å}0\text{Å}0)$ surface during hydrophilic wafer bonding process,” *Mater. Sci. Eng. B* **128**, 93–97 (2006).
 27. G. Chern, I. Lauks, and K. Norian, “Spin-coated amorphous chalcogenide films: photoinduced effects,” *Thin Solid Films* **123**, 289–296 (1985).